IEEE Access
Multidisciplinary | Rapid Review | Open Access Journal

Received December 14, 2017, accepted January 23, 2018, date of publication February 5, 2018, date of current version March 28, 2018.

Digital Object Identifier 10.1109/ACCESS.2018.2802700

Automatic Design and Fabrication of a Custom Ocular Prosthesis Using 3D Volume Difference Reconstruction (VDR)

XIN YE[1], SHAOZE WANG[2], YAN ZHU[3], HUIFENG SHAO[4], LIXIA LOU[1], DAHONG QIAN[5], AND JUAN YE[1]

[1]Department of Ophthalmology, The Second Affiliated Hospital of Zhejiang University, College of Medicine, Hangzhou 310009, China.
[2]Institute of VLSI Design, Zhejiang University, Hangzhou 310027, China.
[3]College of Biomedical Engineering and Instrument Science, Zhejiang University, Hangzhou 310027, China.
[4]State Key Laboratory of Fluid Power Transmission and Control Systems, College of Mechanical Engineering, Zhejiang University, Hangzhou 310027, China.
[5]School of Biomedical Engineering, Shanghai Jiao Tong University, Shanghai 200240, China.

Corresponding authors: Dahong Qian (dahong.qian@sjtu.com.cn) and Juan Ye (yejuan@zju.edu.cn)

This work was supported in part by the National Natural Science Foundation of China under Grant 81670888 and Grant 81471748, in part by the Zhejiang Provincial Program for Medical and Health Science Co-sponsored by Province and Ministry under Grant 2016137996, and in part by the Zhejiang Provincial Program for Cultivation of High-Level Innovative Health Talents.

ABSTRACT We have developed a new computed tomography (CT)-based 3-D volume difference reconstruction (VDR) method for building a model of soft tissue differences using facial self-referenced prototyping computation, and a computer-aided design (CAD) workflow for fabricating custom ocular prostheses (COPs). In facial self-referenced prototyping computation, an ocular prosthesis is constructed from a combination of a top surface, shape contour, and bottom surface, with key measurements being made with respect to the patient's healthy eye. The top surface is derived from the outer region of the healthy eyeball, using Hough transformation. In the meantime, the shape contour and bottom surface are computed from facial edges fitted to Fourier curves. Once these self-referenced parameters have been obtained, finite element analysis is used to generate a primitive prosthesis model. Before being converted into a format suitable for rapid prototyping techniques, the model is refined using surface equations. Oculists choose the final optimized model for printing. Geometric errors, compared with a manually-fabricated prosthesis which has gone through multiple rounds of time-consuming manual adjustment, are as low as 0.46%, and the fabrication time and human error have been greatly reduced. The fill density of the COP is 60%, the wall thickness is 1.6 mm and the weight is 1.59 g. The reconstructed contours and symmetry of the COP are satisfactory with doctors' evaluation and the patient is able to have a normal appearance. The CT-based VDR method we first proposed here can accurately build a model of the soft tissue difference. The full CAD workflow has improved prosthesis design and manufacturing efficiency. This flow can also be applied to other soft issue reconstruction.

INDEX TERMS Computer-aided design, custom ocular prosthesis, computed tomography, self-reference, rapid prototyping.

I. INTRODUCTION

The unfortunate loss of an eye may be caused by trauma, intraocular malignancies, and other serious ocular diseases [1]. Considering the patients' physical and mental health, it is important to correct the ocular disfigurement by wearing prostheses as soon as possible after healing from surgery [2]–[5]. In most cases, an intraorbital implant is placed in the orbital cavity created when the eyeball is completely removed. The intraorbital implant can restore part of the lost volume and an ocular prosthesis which sits on the top of the implant is needed. Custom ocular prostheses (COPs), which are based on individuals' anatomical structure, could fill conjunctival sac and restore aesthetics. Traditional methods to make COPs take a long time to complete due to series of complex steps, which strongly depend on the experience of the oculist [5]. However, there still exists unsatisfactory match between COPs and the patients' conjunctival sac in clinical practice, which may cause pain, secretion, and impaired appearance. Thus, it is meaningful to develop a new approach to fabricate COPs with higher

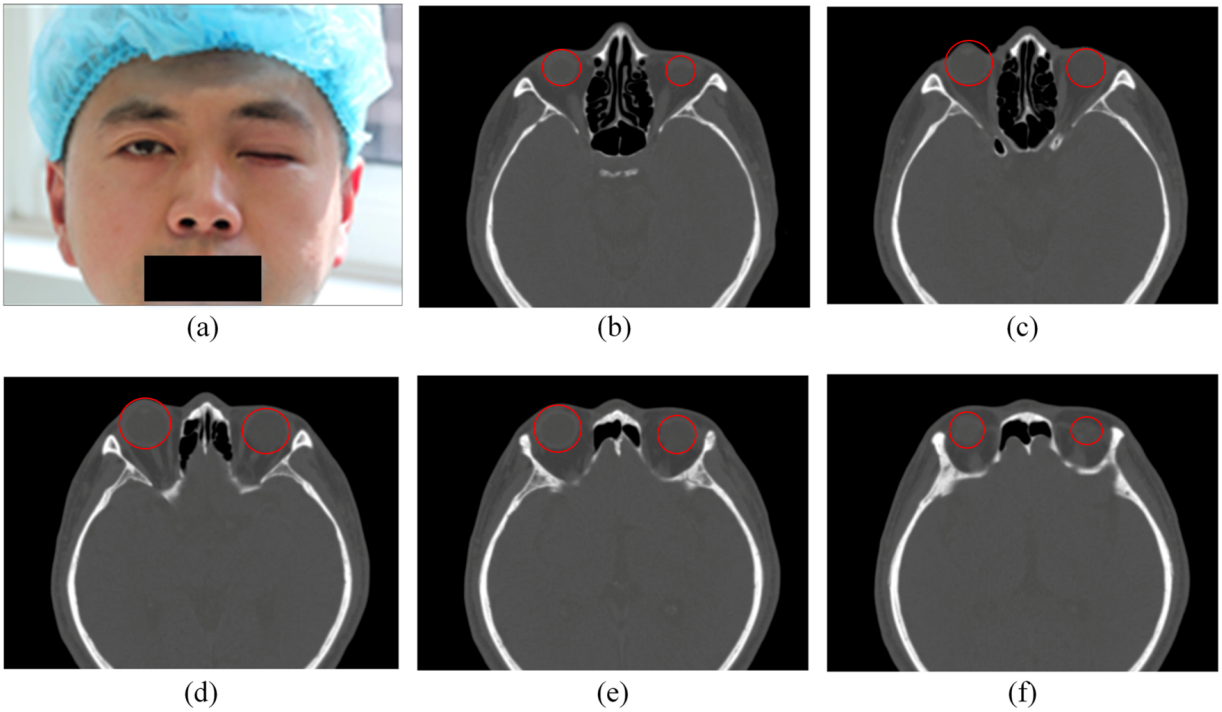

FIGURE 1. Patient without ocular prosthesis (a) and slices containing eyeballs (b)-(f); two red circles on each of (b) – (f) denote outlines of healthy (bigger one) and ocular implant in the damaged socket (smaller one), respectively.

accuracy and efficiency and to fit different anophthalmia sockets.

Following the loss of the globe, the eyelids collapse into the anophthalmic socket and this results in facial asymmetry. Computed tomography (CT) scan can provide detailed information about the anatomical structure in a layered format, clearly delineating the skin surface and the ocular implant. Mirror image techniques, which have been widely used in facial reconstructive surgery, rely on semi-transparent overlays of displaced models that are superimposed onto the original mirror models [6]–[11]. Today, right to left flip methods has been used to find difference on two-dimensional surface in reverse engineering and brain science. However, these techniques cannot directly generate a three-dimensional (3D) model of the volume difference. To solve this problem, we proposed this CT-based 3D volume difference reconstruction (VDR) method for displaying the soft tissue difference using self-referenced computing. Self-reference means that all components of the model are designed with respect to the geometry of the patient's symmetrical fellow eye. Once the self-referenced parameters are obtained, a primitive prosthesis model can be generated using finite element analysis. Rapid prototyping (RP) technique is a promising approach for customizing a product rapidly [12], and is used in this study for fabricating COP.

The quality of the COPs is affected by several important factors, including its shape, size and thickness, as well as the shapes of the anterior and posterior curves. In this study, we introduced the CT-based VDR method for reconstructing a 3D model of conjunctival sac and determining COPs parameters. Combined with RP techniques, a new, faster and more accurate computer-aided design (CAD) workflow for fabricating COP is proposed.

II. MATERIALS AND METHODS

A. DATA COLLECTION SPECIFICATIONS

The proposed COP design workflow takes high-resolution helical CT as its input. CT parameters include, but are not limited to, a slice thickness of no more than 1 mm, image size of 512×512 pixels, and a pixel size no larger than 1 mm. For patients who have lost an eye, customization is the primary concern, and we introduce the new workflow with a specific patient, a 37-year-old who lost his eye through enucleation surgery 11 years ago.

The patient's CT data was collected using a General Electric CT scanner, with 1 mm thickness and 0.36 mm^2 square pixels. Among a total of 115 anonymous slices from the bottom of the head to the top, slice indices from 30 to 74 were extracted as the interesting region for the eyeballs by an ophthalmologist. Fig. 1 illustrates the patient's appearance without ocular prosthesis as well as 5 slices from index 30 to 50 with a step of 5.

B. METHODS

The proposed method regards a custom ocular prosthesis as a combination of a top surface, a projection shape on the z-axis, and a bottom surface, as shown in in Fig. 2. The top surface is derived from the outer surface of the healthy

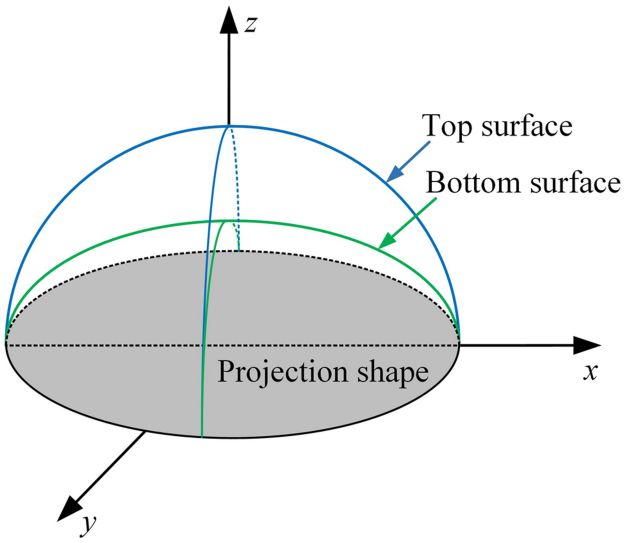

FIGURE 2. Model of a custom ocular prosthesis.

eyeball obtained from Hough transformation [13], [14]. In the meantime, the shape contour and bottom surface are computed from facial edges that are fitted with a cluster of Fourier curves [15]. Measuring parameters for these three components is essential for constructing a digital ocular model. This process is known as reverse engineering (RE). Fig. 3 shows the entire RE process, which involves three components: extracting the top surface, computing the shape and the bottom surface, trimming and rapid prototyping.

1) EXTRACTING TOP SURFACE

When an ocular prosthesis is implanted into a socket, the top surface of the prosthesis must be aligned with the patients' healthy eyeball. Thus, it is necessary to extract parameters from the healthy eyeball, determining its radius and center coordinates. To achieve this, a Hough transformation is employed to detect the circle of the healthy eye on image slices in the interesting region. Hough transformations can detect lines and circles by voting for each parameter's matrix element. For circle detection, the parameter space is three-dimensional, (x_0, y_0) and r records the center coordinates and radii. To reduce computing overhead, only edge pixels are involved as voters. We use a Canny edge detection algorithm, known for its effectiveness. One edge pixel with coordinates (x, y) votes for an element at $(x_0, y_0, \lfloor r \rfloor)$ if and only if

$$(x - x_0)^2 + (y - y_0)^2 = r^2, \quad 1 \leq x_0, \ y_0 \leq 512, \ \lfloor r \rfloor \geq 1 \tag{1}$$

where x_0, y_0 are both integrals and $\lfloor r \rfloor$ is the maximum integral no larger than r.

To make eyeball detection robust, the radius searching range is limited to 5-15 mm, which covers possible eyeball radii. Once circle parameters are obtained for slices (seen in Fig. 1), a series of circles can be drawn on the images. Once the particular slice indices as well as Hough-estimated radius are known, we can interpolate the other transversal radius by fitting the curve

$$\mathrm{r} = \sqrt{r_{max}^2 - z^2} \tag{2}$$

where r_{max} is the maximum radius of the selected slices and z is the slice index from the maximum slice to the both side, which means that $\mathrm{z} = 0, \pm 1, \pm 2, \ldots$ To fit the cure, a least-square-error (LSE) method is deployed.

The upper part of the 3D sphere is shown in Fig. 3. The ocular implant is also reconstructed and moved towards the healthy one along a line segment that connects both center points of the two 3D spheres. In Fig. 3, the smaller sphere beneath the healthy eyeball is the reconstructed ocular implant. Front-end reference means that the top surface of the COP is extracted from the upper hemisphere of the healthy eyeball. The difference of height between the two balls is compensated in the second part of the process.

2) COMPUTING SHAPE AND BOTTOM SURFACE

The shape of an ocular prosthesis is critical because it gives the size of the prosthesis. A custom ocular prosthesis should have a self-referenced shape that makes the patient comfortable. In our design, the self-referenced shape is generated from facial curves, under the assumption that the interior ocular differences between the lost eye and the normal eye change the shape of the exterior surface proportionally. Once the exterior or facial changes are quantified, the interior ocular shape can be derived from them. The question is now quantifying the facial changes between lost-eye side and the normal side. Since the facial surface can be reconstructed from CT images using surface rendering, detecting facial curves is feasible, and they can be interpolated to reconstruct the facial surface.

There are many curve fitting functions such as logistics, exponents and polynomials. The first two classes of function tend to fit points monotonically, whereas the third tends to over-fit, especially when the curves appear sinuous. Fitting with Fourier curves is a powerful tool for handling sinuous curves with little risk of over-fitting, because the curves being fit are periodic. The final fitted curve is expressed a as sum of n-order harmonic functions,

$$\mathrm{f}(x) = a_0 + \sum_{i=1}^{n} [a_i cos\,(i\omega) + b_i sin\,(i\omega)] \tag{3}$$

where ω denotes the fundamental frequency, a_0 the bias coefficient, and $\mathrm{a_i}$, $\mathrm{b_i}(\mathrm{i} \geq 1)$ represents the i^{th} harmonic frequency coefficients. Note that the x-axis (x) runs from left to right and the y-axis (f(x)) runs from bottom to top. To offset patients' head movements, a preprocessing step is needed to register CT images so that two manually-marked corner points on the helical bones are located on a horizontal line. What's more, the central axis of the head in each image slice is perpendicular to this line and crosses the midpoint. A rigid

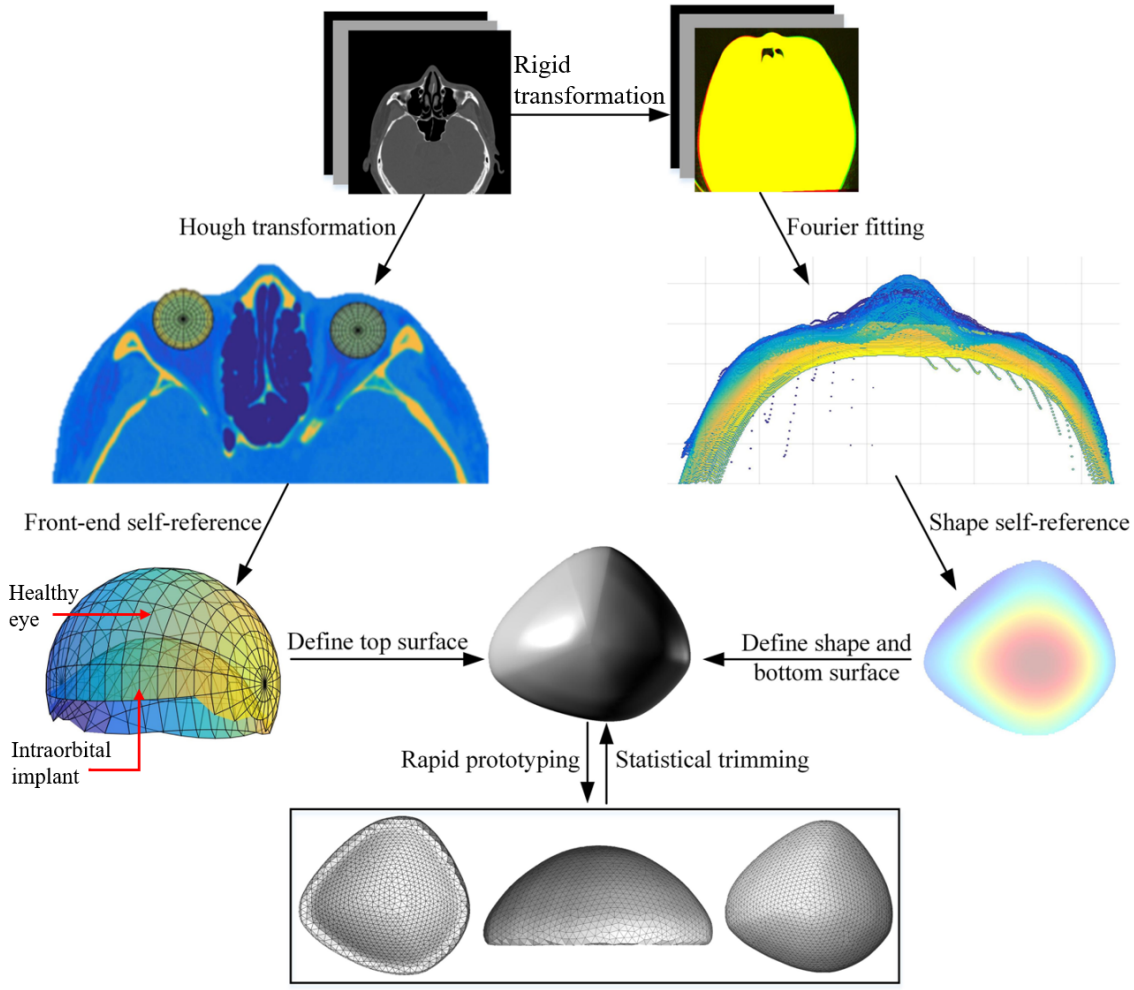

FIGURE 3. Outline of the proposed self-reference custom ocular prosthesis design method.

transformation is adopted:

$$\begin{pmatrix} \mathrm{r}' \\ \mathrm{c}' \\ \mathrm{k} \end{pmatrix} = \begin{pmatrix} \cos\theta & \sin\theta & 1 \\ -\sin\theta & \cos\theta & 1 \\ 0 & 0 & 1 \end{pmatrix} \begin{pmatrix} \mathrm{r} \\ \mathrm{c} \\ \mathrm{k} \end{pmatrix} \tag{4}$$

where r and c denote rows and columns of the original CT images; the upper-script version denotes the registered coordinates. Rotation angle and shift bias are θ and k, respectively. Besides registration on the axial orientation (θ_a and k_a), transformation on coronal orientation θ_c and k_c is also necessary. For our patient, parameters in θ_a, θ_c, k_c and k_a were set to $-1.6°$, 0, 0 and 0, respectively (seen in Fig. 4).

Based on the registered CT data, all slice images are converted into binary images using the OTSU segmentation algorithm, and then a facial contour is detected using a Sobel gradient operator in each slice. Each facial contour curve fitting is done by an 8-order Fourier function, as shown in (3). These Fourier curves allows a facial surface to be plotted with arbitrary up-sampling rates,

$$\mathrm{S} = \left\{ f^i\left(x'\right) | \Delta x' = \Delta x / U, i = 1, 2, \ldots, N \right\} \tag{5}$$

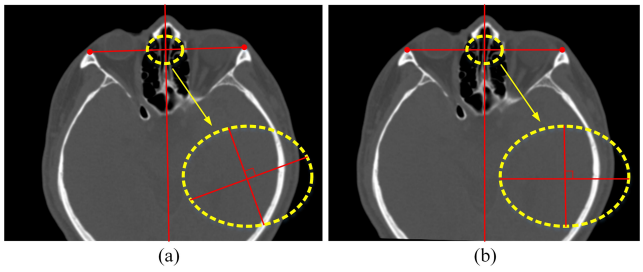

FIGURE 4. Before (a) and after (b) rigid transformation of CT data.

where S denotes the facial surface that is a set of Fourier curves in N slices. Up-sampling rate U is a positive integral which interpolates N-1 points onto a unit interval (Δx). Rendered facial surfaces can be seen in Fig. 3.

Next, primitive bilateral differences are calculated by subtracting the normal-side surface from the damaged side. The two regions are symmetrical across the central axis. Fig. 5(a) shows the differences. Red regions indicate differences that are important for shape extraction. Here the shape contour in

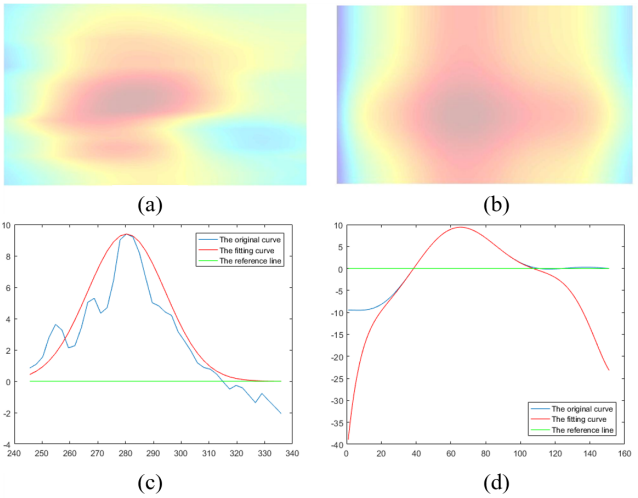

FIGURE 5. Shape model: (a) primitive differences; (b) fitted surface; (c) curve fitting using Gaussian function along the y-axis;(d) curve fitting using polynomial function along the x-axis.

x-y plane is defined as

$$\mathrm{S(x,\,y)} - \mathrm{h} = 0 \tag{6}$$

where h is a free-scale height of a plane vertical against the z-axis. Only points beyond the plane are included in the contour fitting. Here we initialize h with half of the maximum, i.e., $\mathrm{h} = \mathrm{h_{max}}/2$. To solve the contour parameters, a group of equations are built,

$$\begin{cases} S\left(x,\,y\right) = P\left(x\right)G\left(y\right) \\ P\left(x|a_0,\,a_1,\ldots a_7\right) = \sum_{i=0}^{7} a_i x^i \\ G\left(y|\sigma_y,\,c\right) = \dfrac{\mathrm{c}}{\sqrt{2\pi}\sigma_\mathrm{y}} \mathrm{e}^{-\frac{\left(\mathrm{y}-\mu_\mathrm{y}\right)^2}{2\sigma_\mathrm{y}^2}} \\ P\left(\mu_x\right) = G\left(\mu_y\right) = \mathrm{h_{max}} \end{cases} \tag{7}$$

where $\left(\mu_\mathrm{x},\,\mu_\mathrm{y},\,\mathrm{h_{max}}\right)$ denotes the peak point coordinates.

Using (7), a two-dimensional surface is formed using two one-dimensional functions, a Gaussian and a polynomial. Parameters of both functions can be estimated using LSE optimization,

$$\begin{cases} \{\sigma_\mathrm{y},\,\mathrm{c}\} = \mathrm{argmin}\left\{\sum_\mathrm{i}\left(\mathrm{P}(x_i) - \mathrm{z_i}\right)^2,\, y_i = \mu_y\right\} \\ \{a_0,\,a_1,\ldots a_7\} = \mathrm{argmin}\left\{\sum_\mathrm{i}\left(\mathrm{G}(y_i) - \mathrm{z_i}\right)^2,\, x_i = \mu_x\right\} \end{cases} \tag{8}$$

Based on these parameters, the surface S (x, y) as well as the shape contour can be plotted, as shown in Fig. 5(b). The surface equations have one output: the height profile along the z-axis that defines the bottom surface.

3) TRIMMING AND RAPID PROTOTYPING

It's necessary for the size of the custom ocular prosthesis to match the patient's eye width, which means that the height h must be chosen carefully. Suppose the width of a patient's damaged eye is $\mathrm{w_x}$, there is a constraint between w_x and h,

$$\begin{cases} \left|x_l - x_r\right| = w_x \\ S\left(x_l,\,\mu_y\right) = S\left(x_r,\,\mu_y\right) = h \end{cases} \tag{9}$$

where x_l and x_r denote the left and right points along the polynomial curve across the peak point. Once the optimal height is obtained, the shape contour is formed and surface below the contour is cropped out. This first-pass trimmed shape is illustrated in Fig. 6.

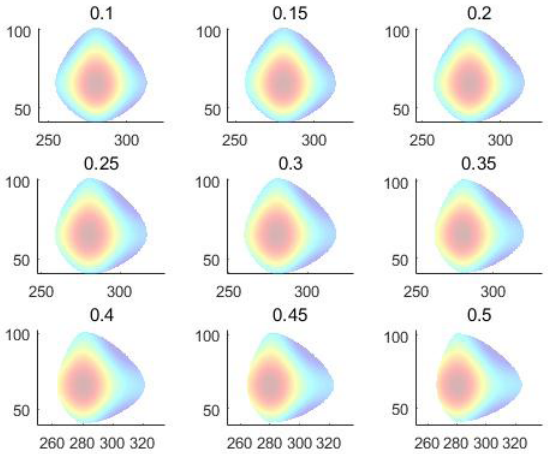

FIGURE 6. Altitude maps of 9 trimmed ocular prosthesis samples with constant k_y. increased from 0.1 to 0.5.

The first trimming only optimizes the shape with respect to the eye width. The shape along the y-axis is also important because the physical construction of a damaged eye tends to require an asymmetrical shape along the y-axis. Hence, y-axis trimming is required to convert the previous symmetrical distribution along the y-axis into an asymmetrical one, whilst keeping the shape along the y-axis (w_y) unchanged. The trimming strategy along the y-axis can be modeled mathematically,

$$\begin{cases} S\left(\mu_x,\,\mu_y - \dfrac{w_y}{2}\right) = S\left(\mu_x,\,\mu_y + \dfrac{w_y}{2}\right) \\ \Delta y = k_y w_y,\, 0 < k_y < 1 \\ \mathrm{S\,(x,\,y)} - \mathrm{h} = 0 \\ \mathrm{x} \in [x_l,\,x_r] \\ y \in \left[\mu_y - \dfrac{w_y}{2} + \dfrac{\Delta y}{2},\, \mu_y + \dfrac{w_y}{2} + \dfrac{\Delta y}{2}\right] \end{cases} \tag{10}$$

Where Δy is the shift distance that is controlled by a ratio constant $\mathrm{k_y}$. To perform a statistical trimming, the constant increase from 0.1 to 0.5, with a step of 0.05 (seen in Fig.6). A doctor can choose the most appropriate shape from these 9 samples. For our patient, the constant was 0.3.

Guided by the combined models of top and bottom surface, and the trimmed shape, a solid model of the ocular prosthesis is created using the Rhinoceros software (version 4.0, USA), as shown in Fig. 7(a) and (b). The model is saved in a stereolithography (STL) file, which is a facet-based representation

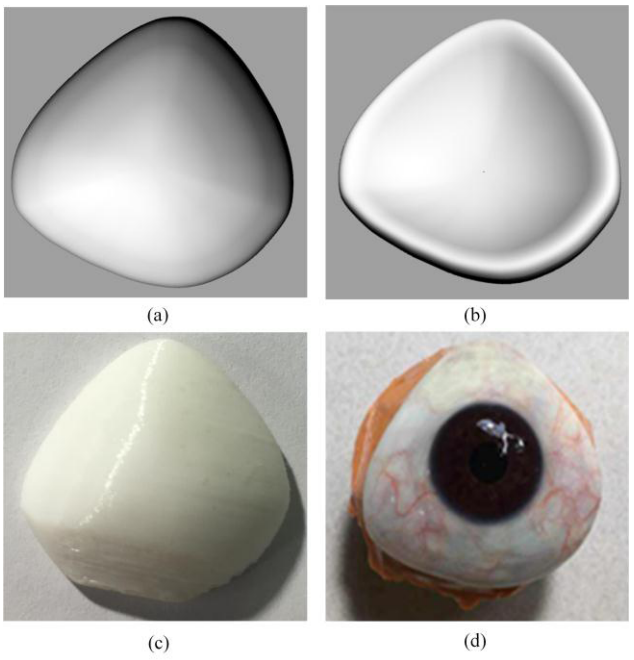

FIGURE 7. Custom ocular prosthesis: (a) top surface of the solid model; (b) bottom surface of the solid model; (c) printed sample; (d) decorated sample.

describing surfaces and solid entities. This file then has been converted into G code to output to a desktop 3D printer [16], using a software slicing tool. A standard polymer filament, Melt Polylactic Acid (PLA) from Shenzhen Esond Technology cooperation, is used for 3D printing. The PLA filament is extruded through a heated metal nozzle at a temperature of 483K, and is deposited onto a receiving station to form the desired prosthesis, as shown in Fig. 7(c). The fill density of the prosthesis and the wall thickness can be altered according to person-specific requirements. The surface is smoothed using a rubber wheel, and the eye is ready for final iris painting and scleral coloring. The iris and pupil are color-matched to the normal eye and the scleral coloring is achieved using oil pigments, as shown in Fig. 7(d).

III. RESULTS

The 3D model of the soft tissue difference was reconstructed for a patient who was referred to our hospital for left COP. The CT-based VDR method was used to evaluate the facial asymmetries effectively. With RP techniques, a new workflow for fabricating COP was developed. A comparison between the geometry of the COP fabricated using our new method and one made using the traditional manual method by an experienced technician was performed and the results are shown in Table 1.

For the top surface, the diameter of the healthy eyeball determined by the Hough transformation is 23.56 mm, and the diameter of the COP is 21.76 mm. The height of the COP is 11.78 mm, which is half of the diameter of the healthy eye ball. The thickness is 7.18 mm, which is defined

TABLE 1. Length and Thickness comparison of COP from the proposed method with traditional handcraft one.

	Traditional (mm)	Proposed (mm)	Difference (mm)	Error (%)
Horizontal maximum length	25.98	26.10	0.12	0.46
Vertical axis maximum length	25.18	26.24	1.06	4.04
Height	10.77	11.78	1.01	9.38
Thickness	7.41	7.18	0.23	3.10

Error = 100% × Difference /Traditional

as the distance from the front surface of the healthy eye ball to that of the ocular implant. For the shape and the bottom surface, the horizontal maximum length of the CAD model is 26.10 mm, and the vertical axis maximum length is 26.24 mm. Geometric errors with respect to the traditional model range from 0.46% to 9.38%. Our COP has a very similar geometry to the COP made using the traditional method (Fig. 8). The fill density of our COP is 60%, the wall thickness is 1.6 mm and the weight is 1.59g. COP fabrication time was greatly reduced when compared to the traditional method.

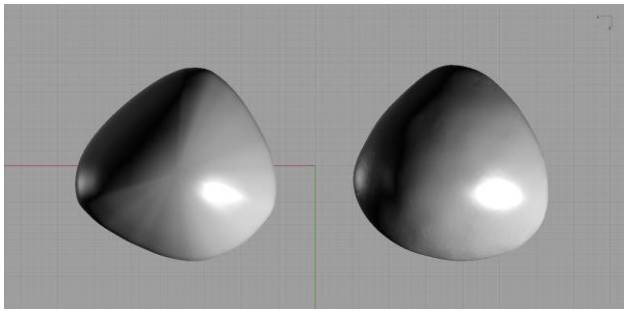

FIGURE 8. The prosthesis designed by the new method (left) and the conventional method (right) have very similar geometries.

The clinical performance of the COP made using our method is good. It was fitted into the patient's conjunctive sac and successfully corrected for the volume deficit and reconstructed the contour. It matched the appearance of the healthy eye and achieved ocular symmetry. The patient was able to have a normal appearance and was satisfied with their COP.

IV. DISCUSSION

Sockets suitable for the self-referenced computing method should have a centered orbital implant, with quiet conjunctiva status and no granulomas. In addition, patients with socket contracture, sulcus deformity or lagophthalmos should be excluded.

Nowadays, RP techniques have been widely used in medical education, surgical planning, and custom implant fabrication [17]–[19]. With RP techniques, a new workflow for fabricating COPs has been developed. The COPs made

using the CAD workflow presents several advantages compared to the traditional workflow. Traditionally, the ocular impression made with impression materials is affected by the patient's cooperation and the technician's experience. The traditional workflow is high-cost and time consuming, involving the following steps and iterations: careful socket fitting, complex handicraft, and long-term consultation with the oculist. In contrast, the CAD workflow is both noninvasive and rapid. It effectively reconstructs the anophthalmic socket defect, decreases treatment time, and requires minimal shape modification. With the help of RP techniques, a COP can be made from digital data and be immediately fitted into the patient's conjunctival sac. Furthermore, reducing the fill density of COPs can reduce the weight, which is helpful in reducing the eye lid laxity complication associated with heavy prostheses.

This paper first proposed CT-based Volume Difference Reconstruction (VDR) method for building 3D models of the soft tissue differences using self-referenced. This technique can be a powerful tool for other clinical uses such as reconstructing body parts based on body symmetry and/or finding tissue difference quantitatively over time. In traditional clinical practice, several bilateral anatomical facial landmarks are defined on 3D CT images and their distances from the mid-facial symmetry plane are used to evaluate the asymmetry index of each of the landmarks [10], [17], [20]–[24]. The main problems with manual measurements are that they can only be estimated reliably for a small number of points, and they are also unable to provide 3D models of the facial surface differences. Our CT-based VDR method solves both the problems. The ocular defect model is reconstructed directly and accurately because the surface of the patient's bilateral eye is efficiently fit by an analytical expression and the difference is calculated on each CT slice. Analytical expressions can give better accuracy than traditional techniques such as direct volume rendering or surface-based rendering [25]. Self-reference means that the 3D volume reference data is calculated with respect to the geometry of a patient's normal eye. Then difference data is incorporated into an accurate 3D defect model.

Limitations of this study include its restriction to a single patient and the non-opaque layer materials used in COP. Future work may focus on improving CAD processes and researching improved materials. Geometric errors on our COP, compared to the one made using the traditional errors are a minimum of 0.46%. There are two main error sources. First, when computing the bottom surface, the surface equations generate a single by-product: the height profile along z-axis which defines the bottom surface. However, the broad characteristics of the shape of the ocular prosthesis should be taken into consideration when choosing the optimal z-axis value. Thus, the design of the bottom surface is semi-automatic process that is affected by the oculist's aesthetic standards. Second, skin laxity of the anophthalmic side eyelid might slightly affect the bilateral soft tissue difference. With loss of support after enucleation, the eyelids collapse into the anophthalmic socket and cause skin laxity. The currently proposed VDR techniques are expected to be adapted to the imaging data from more patients in the future.

CT-based VDR techniques provide 3D shape data that can be used to repair facial defects and have other potential clinical applications. RP techniques have not been widely used in ophthalmology but a good understanding of these techniques may be beneficial to ophthalmologists. Self-referenced computing technique can be used to evaluate right-left differences in asymmetrical defects of patients by subtracting the volume of soft tissue on the deformity side from the healthy side. This proposed technique can also provide insights for clinic treatment planning in reconstruction surgery for orbitozygomatic fractures, mandibular deformity, skull repair, nasal defect restoration, and breast plastic surgery, etc. Self-referenced computing techniques might also allow a quantitative evaluation of treatment effectiveness in following-up patients.

ACKNOWLEDGMENT

The authors acknowledge Tianye Niu at Zhejiang University, China and In Chi Sung at Kim's Eye Hospital, Korea and Seong Hyeon Ki at Kim's Eye Hospital, Korea and Kechun Zhu at University of Toronto, Canada for their help.

Disclosure: X. YE, None; S.Z. WANG, None; Y. ZHU, None; H.F. SHAO, None; L.X. LOU, None; D.H. QIAN, None; J. Ye, None.

REFERENCES

[1] K. R. Pine, B. H. Sloan, and R. J. Jacobs, "The anophthalmic patient," in *Clinical Ocular Prosthetics*. Cham, Switzerland: Springer, 2015, pp. 10–13.

[2] K. Pine, B. Sloan, J. Stewart, and R. J. Jacobs, "Concerns of anophthalmic patients wearing artificial eyes," *Clin. Experim. Ophthalmol.*, vol. 39, no. 1, pp. 47–52, 2010.

[3] I.-I. Artopoulou, P. C. Montgomery, P. J. Wesley, and J. C. Lemon, "Digital imaging in the fabrication of ocular prostheses," *J. Prosthetic Dentistry*, vol. 95, no. 4, pp. 327–330, 2006.

[4] E. Kale, A. Meşe, and A. D. Izgi, "A technique for fabrication of an interim ocular prosthesis," *J. Prosthodontics-Implant Esthetic Reconstructive Dentistry*, vol. 17, no. 8, pp. 654–661, 2008.

[5] K. Raizada and D. Rani, "Ocular prosthesis," *Contact Lens Anterior Eye*, vol. 30, no. 3, pp. 152–162, 2007.

[6] S. J. Lee, H. P. Lee, K. M. Tse, E. C. Cheong, and S. P. Lim, "Computer-aided design and rapid prototyping-assisted contouring of costal cartilage graft for facial reconstructive surgery," *Craniomaxillofacial Trauma Reconstruction*, vol. 5, no. 2, pp. 75–82, 2012.

[7] K. M. Van Lierde *et al.*, "Speech characteristics one year after first Belgian facial transplantation," *Laryngoscope*, vol. 124, no. 9, pp. 2021–2027, 2014.

[8] M. A. R. Kuijpers, Y.-T. Chiu, R. M. Nada, C. E. L. Carels, and P. S. Fudalej, "Three-dimensional imaging methods for quantitative analysis of facial soft tissues and skeletal morphology in patients with orofacial clefts: A systematic review," *PLoS ONE*, vol. 9, no. 4, p. e93442, 2014.

[9] E. De Momi *et al.*, "Automatic extraction of the mid-facial plane for cranio-maxillofacial surgery planning," *Int. J. Oral Maxillofacial Surg.*, vol. 35, no. 7, pp. 636–642, 2006.

[10] M. Y. Hajeer, A. F. Ayoub, and D. T. Millett, "Three-dimensional assessment of facial soft-tissue asymmetry before and after orthognathic surgery," *Brit. J. Oral Maxillofacial Surg.*, vol. 42, no. 5, pp. 396–404, 2004.

[11] L. H. Cevidanes *et al.*, "Three-dimensional quantification of mandibular asymmetry through cone-beam computerized tomography," *Oral Surg., Oral Med., Oral Pathol., Oral Radiol., Endodontics*, vol. 111, no. 6, pp. 757–770, 2011.

[12] W.-Y. Yeong, C.-K. Chua, K.-F. Leong, and M. Chandrasekaran, "Rapid prototyping in tissue engineering: Challenges and potential," *Trends Biotechnol.*, vol. 22, no. 12, pp. 643–652, 2004.
[13] N. Thomae, K. U. Plagwitz, P. Husar, and G. Henning, "[Hough transformation for image processing in eye tracking recording]," *Biomed. Tech. Biomed. Eng.*, vol. 47, no. Suppl 1, pp. 636–638, 2002.
[14] O. Ecabert *et al.*, "Automatic model-based segmentation of the heart in CT images," *IEEE Trans. Med. Imag.*, vol. 27, no. 9, pp. 1189–1201, Sep. 2008.
[15] C. M. de Bazelaire, G. D. Duhamel, N. M. Rofsky, and D. C. Alsop, "MR imaging relaxation times of abdominal and pelvic tissues measured *in vivo* at 3.0 T: preliminary results," *Radiology*, vol. 230, no. 3, pp. 652–659, 2004.
[16] A. Liu *et al.*, "3D printing surgical implants at the clinic: A experimental study on anterior cruciate ligament reconstruction," *Sci. Rep.*, vol. 6, no. 1, 2016, Art. no. 21704.
[17] W. Huang and X. Zhang, "3D printing: Print the future of ophthalmology," *Investigat. Ophthalmol. Vis. Sci.*, vol. 55, no. 8, pp. 5380–5381, 2014.
[18] Y. He, G.-H. Xue, and J.-Z. Fu, "Fabrication of low cost soft tissue prostheses with the desktop 3D printer," *Sci. Rep.*, vol. 4, Nov. 2014, Art. no. 6973.
[19] H. H. L. Chan, J. H. Siewerdsen, A. Vescan, M. J. Daly, E. Prisman, and J. C. Irish, "3D rapid prototyping for otolaryngology—Head and neck surgery: Applications in image-guidance, surgical simulation and patient-specific modeling," *PLoS ONE*, vol. 10, no. 9, p. e0136370, 2015.
[20] K. Bajaj, P. Rathee, P. Jain, and V. R. Panwar, "Comparison of the reliability of anatomic landmarks based on PA cephalometric radiographs and 3D CT scans in patients with facial asymmetry," *Int. J. Clin. Pediatric Dentistry*, vol. 4, pp. 213–223, 2011.
[21] V. F. Ferrario, C. Sforza, J. H. Schmitz, and F. Santoro, "Three-dimensional facial morphometric assessment of soft tissue changes after orthognathic surgery," *Oral Surg., Oral Med. Oral Pathol., Oral Radiol. Endodontics*, vol. 88, no. 5, pp. 549–556, 1999.
[22] R. Manara *et al.*, "Facial asymmetry quantitative evaluation in oculoauriculovertebral spectrum," *Clin. Oral Investigat.*, vol. 20, no. 2, pp. 219–225, 2016.
[23] E. Guest, E. Berry, and D. Morris, "Novel methods for quantifying soft tissue changes after orthognathic surgery," *Int. J. Oral Maxillofacial Surg.*, vol. 30, no. 6, pp. 484–489, 2001.
[24] M. Maeda *et al.*, "3D-CT evaluation of facial asymmetry in patients with maxillofacial deformities," *Oral Surg., Oral Med., Oral Pathol., Oral Radiol., Endodontics*, vol. 102, no. 3, pp. 382–390, 2006.
[25] F. Gremse, M. Stärk, J. Ehling, J. R. Menzel, T. Lammers, and F. Kiessling, "Imalytics preclinical: Interactive analysis of biomedical volume data," *Theranostics*, vol. 6, no. 3, pp. 328–341, 2016.

XIN YE was born in Hangzhou, China. She received the M.D. degree from the College of Medicine, Zhejiang University, China, in 2015. She is currently pursuing the Ph.D. degree with the Department of Ophthalmology, The Second Affiliated Hospital of Zhejiang University, College of Medicine, China. Her current research interests include ophthalmology, biomedical engineering, and translational Medicine.

SHAOZE WANG was born in Anhui, China. He received the B.S.E. degree from Hangzhou Dianzi University, Zhejiang, China, in 2012, and the Ph.D. degree from the Institute of VLSI Design, Zhejiang University, in 2017. He is currently an Algorithm Engineer with the Hangzhou Department, Arcsoft Company, China. His current research interests include computer vision, biomedical engineering, and image quality assessment.

YAN ZHU received the B.E. degree from the School of Data and Computer Science, Sun Yat-sen University, China, in 2016. She is currently pursuing the Ph.D. degree with the Key Laboratory of Biomedical Engineering, Zhejiang University. Her research interests include bioinformatics and deep learning for biomedical application.

HUIFENG SHAO was born in Zhejiang, China. He received the B.E. degree from the Zhejiang University of Technology, Hangzhou, China, in 2012, the Ph.D. degree from the School of Mechanical Engineering, Zhejiang University, in 2017. He is currently a Post-Doctoral Fellow with Zhejiang University. His current research interests include 3-D printing, biomedical engineering, biofabrication, and bone regeneration.

LIXIA LOU received the bachelor's degree in psychology and the M.D. degree in clinical medicine from Zhejiang University, China. She is currently a Clinical Resident with The Second Affiliated Hospital of Zhejiang University. Her current research interest is the epidemiology of eye diseases, including cataract, macular degeneration, and refractive error.

DAHONG QIAN was born in Shanghai, China. He received the B.S.E. degree from Zhejiang University, Zhejiang, China, in 1988, the M.S.E. degree from The University of Texas at Austin, TX, USA, in 1991, and the Ph.D. degree in computer science from Harvard University, Cambridge, MA, USA, in 2002. Since 1992, he has been holding various engineering and management positions at Dallas Semiconductor/Maxim, Analog Devices, and OmniVision. He was also the co-founder of several startup companies. He is a currently a Professor with the School of Biomedical Engineering, Shanghai Jiao Tong University.

JUAN YE received the M.D. degree from Zhejiang University, China, and the Ph.D. degree from Yonsei University, South Korea. She is currently a Professor with the Department of Ophthalmology, The Second Affiliated Hospital of Zhejiang University, and the Deputy Director of the Chinese Society of Oculoplastic Surgery and Orbital Disease. Her current research interests include treatment of eyelid deformity, orbital reconstruction, and epidemiology of age-related eye disease.